

High-throughput sorting of drops in microfluidic chips using electric capacitance

Arjen M. Pit, Riëlle de Ruiter, Anand Kumar, Daniel Wijnperlé, Michèl H. G. Duits, and Frieder Mugele

Citation: [Biomicrofluidics](#) **9**, 044116 (2015); doi: 10.1063/1.4928452

View online: <http://dx.doi.org/10.1063/1.4928452>

View Table of Contents: <http://scitation.aip.org/content/aip/journal/bmf/9/4?ver=pdfcov>

Published by the [AIP Publishing](#)

Articles you may be interested in

[A high-throughput cellulase screening system based on droplet microfluidics](#)

[Biomicrofluidics](#) **8**, 041102 (2014); 10.1063/1.4886771

[Microarray of non-connected gold pads used as high density electric traps for parallelized pairing and fusion of cells](#)

[Biomicrofluidics](#) **7**, 044101 (2013); 10.1063/1.4813062

[High-throughput particle manipulation by hydrodynamic, electrokinetic, and dielectrophoretic effects in an integrated microfluidic chip](#)

[Biomicrofluidics](#) **7**, 024106 (2013); 10.1063/1.4795856

[A microfluidics approach towards high-throughput pathogen removal from blood using margination](#)

[Biomicrofluidics](#) **6**, 024115 (2012); 10.1063/1.4710992

[Reduction of water evaporation in polymerase chain reaction microfluidic devices based on oscillating-flow](#)

[Biomicrofluidics](#) **4**, 036502 (2010); 10.1063/1.3481776

Did your publisher get
18 MILLION DOWNLOADS in 2014?
AIP Publishing did.



THERE'S POWER IN NUMBERS. Reach the world with AIP Publishing.



High-throughput sorting of drops in microfluidic chips using electric capacitance

Arjen M. Pit,^{a)} Riëlle de Ruiter, Anand Kumar, Daniel Wijnperlé,
Michèl H. G. Duits, and Frieder Mugele
*Physics of Complex Fluids Group, MESA+ Institute, University of Twente,
P.O. Box 217, 7500 AE Enschede, The Netherlands*

(Received 15 June 2015; accepted 30 July 2015; published online 10 August 2015)

We analyze a recently introduced approach for the sorting of aqueous drops with biological content immersed in oil, using a microfluidic chip that combines the functionality of electrowetting with the high throughput of two-phase flow microfluidics. In this electrostatic sorter, three co-planar electrodes covered by a thin dielectric layer are placed directly below the fluidic channel. Switching the potential of the central electrode creates an electrical guide that leads the drop to the desired outlet. The generated force, which deflects the drop, can be tuned via the voltage. The working principle is based on a contrast in conductivity between the drop and the continuous phase, which ensures successful operation even for drops of highly conductive biological media like phosphate buffered saline. Moreover, since the electric field does not penetrate the drop, its content is protected from electrical currents and Joule heating. A simple capacitive model allows quantitative prediction of the electrostatic forces exerted on drops. The maximum achievable sorting rate is determined by a competition between electrostatic and hydrodynamic forces. Sorting speeds up to 1200 per second are demonstrated for conductive drops of 160 pl in low viscosity oil. © 2015 AIP Publishing LLC.
[\[http://dx.doi.org/10.1063/1.4928452\]](http://dx.doi.org/10.1063/1.4928452)

I. INTRODUCTION

In the past decade, droplet microfluidics has matured from “having great potential” to real-life applications.¹ Small drops used as micro reactors require minute amounts of reaction material while fast drop generation allows for numerous samples in a short time. A topic of high interest in the field is the analysis of biological cells encapsulated in drops. Drops provide an attractive means to separate a cell from its surroundings and assess its individual characteristics. These include not only markers that are localized on the cell membrane but also concentrations of biomolecules excreted by the living cell or released after cell lysis. Such applications often involve large populations (thousands to millions) of cells, implying the generation and inspection of at least an equal number of drops. While significant progress has been made in handling such staggering numbers of drops,² there are also several issues remaining that still need to be addressed.

One of these issues is obtaining populations of drops, which all contain one cell. Simply generating drops from a cell suspension leads to distributions in the occupancy per drop: empty, single, double, etc., due to the inherent Poisson statistics. The concentration of the cell suspension and the volume of the drops then determine the relative probabilities.³ One approach to circumvent this issue has been to passively arrange the cells before injection. Techniques like close-packed ordering³ and Dean flow ordering⁴ have been applied with some success, but do require fine-tuning of oil flows and the final cell-in-drop population is not 100% for prolonged periods of time.

^{a)} Author to whom correspondence should be addressed. Electronic mail: a.m.pit@utwente.nl

An alternative, and potentially more reliable, approach is to actively sort out drops that contain only one cell. To this end, several techniques have been developed, for instance, sorting based on contrast in permittivity (dielectrophoresis, DEP),^{5,6} the use of surface acoustic waves (SAW),⁷ using pressure pulses,⁸ electrically pre-charging the drops,⁹ laser induced sorting,¹⁰ and the use of membrane valves.¹¹ A drawback of all these methods is that the number of drops to be sorted is even higher than the already staggering number of cells: in a typical injection of a cell suspension, the average occupancy per drop is often in the range of 0.1–0.2. Clearly, this prompts the need for high sorting speed devices.

A second issue concerns the reliability of the drop manipulation. Even if each of the drops already contains one cell, they still need to be analyzed at a specific on-chip location or transported to a specific outlet with high probability of success and without damage along the path.

Recently, we presented a drop manipulation method, which combines the functionality of electro-wetting-on-dielectric (EWOD) with the high throughput of two-phase flow microfluidics by integrating insulated electrode geometries just below the microchannel. The method can, besides trapping, releasing, splitting, and guiding, also perform sorting of drops in flow.¹² It is highly promising, because of (i) on-demand and fast actuation: electric fields can be switched rapidly, unlike mechanical valves or pressures, (ii) non-invasiveness: the electric field does not penetrate the drop and therefore causes no (potentially harmful) Joule heating, (iii) ease and flexibility of design, and (iv) ability to predict the electrostatic force based on a capacitive model. This technique, however, only showed sorting rates of 25 drops per second and has not been translated to a practical drop sorter.

The present paper focuses on the reliability and speed of sorting, while also durability and biocompatibility are considered. In particular, we discuss the capabilities of a sorter similar to one that was recently introduced¹² and has since then been improved to allow sorting at 1200 drops per second. The performance of the sorter is characterized. First, the theoretical dependence of the sorting force on the actuation voltage and drop size is explored. We show that the electrostatic and hydrodynamic forces on the drop can be estimated with reasonable accuracy from analytical models and used to predict the required sorting conditions. Subsequently, several working points around this condition are explored, to ascertain the quantitative requirements for >99% sorting efficiency.

We demonstrate the performance of our sorter via different experiments. We show that the use of highly conductive liquids, like phosphate buffered saline, do not pose any limitations to the ability to sort drops, thus opening the road to its use for biological applications. We show that sorting speeds as high as 1200 drops per second can be achieved by using a low viscosity oil. Finally, we also report preliminary results of active sorting on demand, using fluorescence based detection of cells in drops, achieving a rate of 400 drops per second.

II. MATERIALS AND METHODS

The setup for generating and sorting drops in ambient oil is illustrated in Fig. 1. In a 50 μm high microchannel, drops are generated via a flow focusing device (FFD) with a 50 μm wide orifice. Water drops are formed in the continuous oil phase consisting of Fluorinert FC-40. The generated drops are squeezed between the top and bottom wall of the microchannel.

The pressures of the oil and water phases are separately adjusted by a custom written Labview program, which drives a home-made pressure controller consisting of two pressure regulators and three-way solenoid valves. The air pressure difference (ΔP) of the two closed vials containing water or oil can be independently regulated from 1 to 100 kPa. The drop radius, speed, and inter-drop distance can be tuned via the magnitudes and ratio of the oil and water phase pressures. The oil flow rate can be set from 0 to ~ 10 ml/h, corresponding to average velocities of 0 to ~ 40 cm/s in the main channel. The drop radii can be varied from around 25 μm to 60 μm , and the drop generation frequency f_{drop} can be altered from 0 to 2500 drops per second. The pressure controller allows to create single drops on demand by applying a pressure pulse of chosen duration (Δt) and magnitude (ΔP) to the water phase or it can create drops continuously by setting an overpressure to the water phase.

An inverted microscope in combination with a high speed camera is used to visualize and record the sorting events. Matlab scripts are used to identify, which outlet channel is taken by

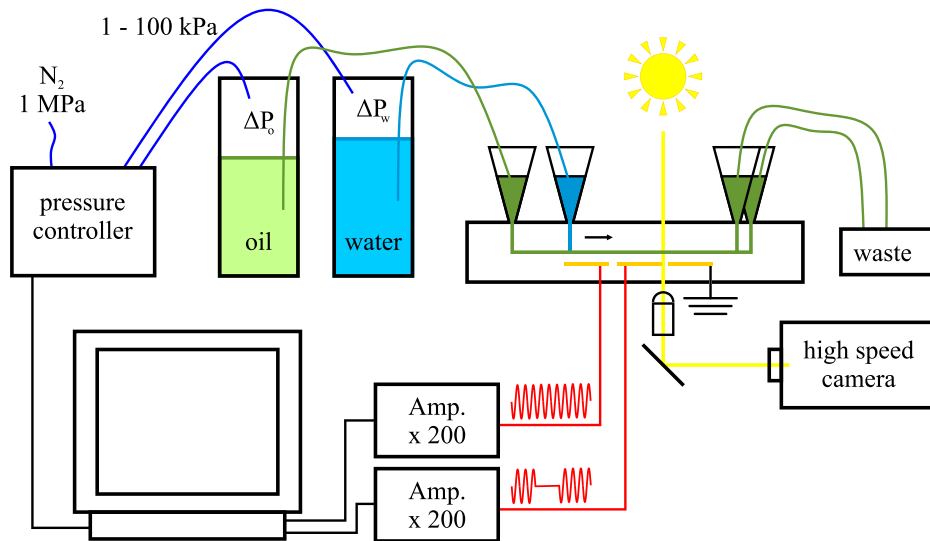


FIG. 1. Schematic overview of the experimental setup. DAQ cards in the computer send two sine waves to two amplifiers attached to the electrodes on the microchip. The computer also controls the pressure of two closed vials—one containing water and the other oil—which allows to control the drop generation and flow rates at the flow focusing device in the chip. A microscope and high speed camera are used to capture the drops passing the electrodes in the channel at 5000 fps.

individual drops, and to extract parameters like drop radius, inter-drop distance, drop generation frequency, and drop velocity from the video recordings. We also measure the position dependent overlap of the droplet with each electrode.

In Figs. 2(a) and 2(b), a top-view of the microfluidic device is shown. Polydimethylsiloxane (PDMS) microchannels are molded using standard soft lithography techniques.¹³ Electrode patterns are etched in an indium tin oxide (ITO) coated glass substrate using an 18% HCl solution.

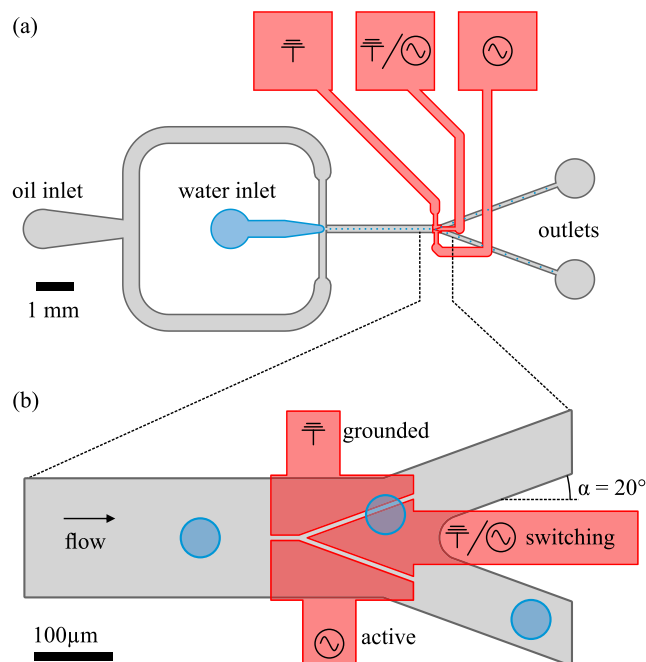


FIG. 2. (a) Schematic overview of the microchannel geometry and the electrode structures incorporated beneath it. (b) Detailed view of the sorter region showing the three-electrode geometry and which electrode is active, grounded, or switching between active and ground state.

Atop the electrodes, a PDMS layer of approximately $3\ \mu\text{m}$ is created by spin coating $600\ \mu\text{l}$ of PDMS at $6000\ \text{rpm}$ for $600\ \text{s}$. This thin layer is partially cured at 65°C for $20\ \text{min}$. Using a stereomicroscope, the electrode structure with partially cured layer is aligned with a previously fabricated PDMS microchannel. After alignment, the curing process is completed at 65°C for another hour to form a permanent seal between the channel and electrode substrate. The thin PDMS layer not only helps sealing the chip but also serves as the dielectric required to insulate the drop from the electric currents.

Sorting takes place $3\ \text{mm}$ downstream from the FFD where a set of 3 electrodes is aligned underneath the channel in front of a symmetric Y-shaped channel junction. The gap between the electrodes was designed to be $10\ \mu\text{m}$, i.e., significantly larger than twice the thickness of the dielectric layer, to prevent short circuiting. Drops are guided towards the desired outlet by switching the center electrode. This is done via a custom made Labview program that generates two in-phase AC sine waves. One of the generated AC signals is modulated with a square pulse (from 0 to 1) for a duration of $\frac{1}{f_{\text{drop}}}$, effectively switching the signal between grounded and active state. This modulated wave is sent towards the switching electrode. The unaltered signal is continuously sent to the bottom electrode, which is always active. Both signals are pre-amplified 200 times by an AC amplifier. The top electrode is continuously grounded (Fig. 2(b)).

Besides the active sorting of uniform drops, which we perform to assess the capabilities and limitations of the sorter, also the sorting of drops with and without cells is explored. To this purpose, a microscope is additionally equipped with a $488\ \text{nm}$ diode laser, of which the beam is expanded using a cylindrical lens and launched into the back aperture of a $40\times$ objective, effectively illuminating a thin slice perpendicular to the channel direction. Emitted light from the fluorescently labeled cells is collected with the same objective, filtered, and detected with a photomultiplier tube (PMT). A reconfigurable data acquisition card (PCIe-7842R) is used to acquire the PMT signal and generate a sorting pulse if a preset threshold is exceeded. The sorting pulse is further amplified with a high-voltage amplifier and sent to the center sorting electrode, effectively sorting single cell-containing drops from empty drops.

III. THEORY

Our microchip functions in the low Reynolds number regime ($\text{Re} < 10$). Therefore, inertia can be neglected. Whether a drop will be sorted or not depends on the balance between the hydrodynamic drag force F_{drag} from the surrounding oil phase and the electrostatic force F_e caused by the voltage that is applied to the electrodes.

The working principle of our electrostatic sorter is analogous to that of the electrostatic traps previously reported for millimetric sessile drops.¹⁴ It can be easily understood by considering our co-planar electrodes as an electrical circuit consisting of two capacitors in series, as drawn in Fig. 3(b). The electrostatic energy of a capacitor in an electric circuit that includes a voltage source is given by¹⁵

$$W_c = -\frac{1}{2}C_{\text{tot}}U^2, \quad (1)$$

where C_{tot} is the total capacitance and U is the root-mean-square of the applied AC voltage. If the channel is filled only with oil, the system has a low intrinsic capacitance originating from the co-planar electrodes surrounded by the $3\ \mu\text{m}$ layer of PDMS and the oil. Substituting the oil above the electrodes with a conductive liquid, the representative electrical circuit changes into a set of two capacitors in series, namely, the two insulating layers of PDMS. If the drop moves over the electrode gap (Fig. 3(c)), the total capacitance is dependent on the areas of the drop above each electrode, A_1 and A_2 ,

$$C_{\text{tot}} = \frac{C_1 C_2}{C_1 + C_2} = c \frac{A_1 A_2}{A_1 + A_2}, \quad \text{with } c = \frac{\epsilon_0 \epsilon_r}{d}, \quad (2)$$

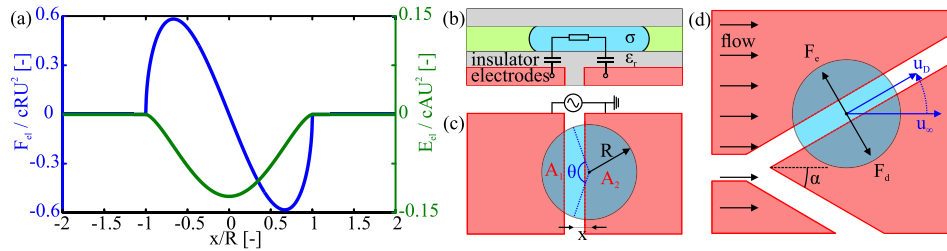


FIG. 3. (a) Non-dimensionalised graphs of the electrostatic potential well (green) and the resulting electrostatic force (blue) exerted on the drop as it traverses the gap, calculated from the analytical two-capacitors-in-series model, plotted against the normalized distance x/R , with x as the distance between the center of mass of the drop and the centerline of the electrode gap. (b) Side view and (c) top view of a drop covering two electrodes with an applied potential difference. For conductive drops with negligible Ohmic resistance, the whole system can be considered as two capacitors in series. (d) A drop undergoing sorting. Under the influence of the electrostatic force, the velocity vector of the drop decreases in magnitude and changes direction. In equilibrium, the drag force opposes the electrostatic force and the drop moves at constant velocity over the gap.

with ϵ_r being the relative permittivity of PDMS, and d being the thickness of the insulating layer. For a typical water drop (with radius $R = 30 \mu\text{m}$) centered above an electrode gap of $10 \mu\text{m}$, the capacitance increases from 0.7 to 4.1 fF, when the water displaces the oil. The total electrostatic energy gain as a drop moves across the electrodes (Fig. 3(c)) thus becomes

$$W_e = -\frac{1}{2} \frac{\epsilon_0 \epsilon_r}{d} \frac{A_1 A_2}{A_1 + A_2} U_{tot}^2. \quad (3)$$

It is therefore energetically favorable to exchange the oil with water, and this energy gain increases with the square of the applied potential. The electrostatic force that is exerted when the drop moves perpendicular to the gap can be calculated by taking the derivative with respect to the drop displacement x ,

$$F_e = -\frac{dW_e}{dx} = \frac{\epsilon_0 \epsilon_r}{\pi d} U_{tot}^2 R \sin\left(\frac{\theta}{2}\right) (\pi + \sin(\theta) - \theta), \quad \text{with } \theta = 2 \cos^{-1}\left(\frac{x}{R}\right). \quad (4)$$

In Fig. 3(a), the non-dimensionalised electrostatic energy and force landscapes are plotted against the distance between the drop's center-of-mass and the center of the gap. The net electrostatic force is always perpendicular to the gap between the electrodes. In practice, this means that the drop will always try to center itself on the gap. External forces, like the drag force, will be opposed by this electrostatic force as the drop is pushed away from the gap, leading to either a new equilibrium position, or release from the electrodes if the external force exceeds the maximum trapping force. From the analytical formula for F_e , we can numerically determine that the maximum force is exerted when the drop is located at $x \sim 0.67R$. Thus, the electrostatic force has a maximum amplitude of

$$F_{el,max} = 0.58 \frac{\epsilon_0 \epsilon_r}{d} U^2 R. \quad (5)$$

This expression for the maximum force has been validated using a capillary force sensor.¹⁶

Previously,¹² we analytically approximated the hydrodynamic drag force F_d on a stationary drop by modelling the drop as a (cylindrical) pillar with no-slip boundary conditions in an infinitely wide channel. Since the drop diameter is about one third of the channel width w , we chose to neglect the effect of the channel walls on the drag force. This yields

$$F_d = \left(\frac{24\pi\mu u_{oil} R^2}{h} \right) \left(1 + \frac{2K_1(q)}{qK_0(q)} \right), \quad (6)$$

with μ as the viscosity of the oil, u_{oil} as its velocity, R as the pillar (i.e., drop) radius, h as the channel height, and K_1 and K_2 as modified Bessel functions of the second kind with

$q = 2\sqrt{3}R/h$. We also assume a constant oil velocity in the center region of the channel. For a moving drop, we can then replace u_{oil} by the relative velocity $\Delta u = u_{oil} - u_{drop}$.

Another factor that is of importance for the sorting operation is the inclination angle α of the Y-junction of the sorting electrodes (Fig. 3(d)). Before reaching the sorting geometry, the drop moves at constant velocity through the channel. The net force on the drop is zero, because viscous dissipation and drag are balanced. Under the action of the electrostatic force, the velocity vector decreases in magnitude and changes direction. The drag force adapts to this change in velocity until a new steady state is reached and the drop moves at a constant velocity over the gap between the electrodes. From a simple force balance (Fig. 3(d)), at constant drop velocity in the direction of the gap, we find that the requirement for a drop to stay on the gap is $F_{e,max} \geq F_d \sin(\alpha)$. The smaller the inclination angle, the easier sorting should be. The total length of the electrode geometry is limited by the inter drop distance, because a consecutive drop should not be influenced by the voltage applied for the sorting of the previous drop. As a compromise between size and low inclination angle, an angle of 20° was chosen.

Equation (5) provides an estimate of the forces acting on a water drop during sorting. For example, the maximum possible electrostatic force exerted on a drop in FC-40 is $F_{el,max} = 5.2 \mu\text{N}$ (given $R = 30 \mu\text{m}$, $\epsilon_r \sim 2.1$, $d = 3 \mu\text{m}$, $U = 220 V_{RMS}$). This simple formula, however, does not take into account the $10 \mu\text{m}$ gap between the electrodes. A numerical calculation including the gap shows a 20% reduction to $F_{el,max} = 4.1 \mu\text{N}$. This force calculated from the model is quite accurate.^{12,16} In practice, the largest errors result from determination of the drop radius from experimental images, and the uncertainty in the dielectric thickness, which not only comprises the thin PDMS layer but also of a thin layer of dynamically entrapped oil which alters with different experimental parameters.¹⁷

In experiments aimed at finding the maximum sorting speeds for drops in FC-40 (Fig. 5), we estimate Δu to be $\sim 0.2 \text{ m/s}$, which, from Eq. (6), results in $F_{drag} \sim 1.2 \mu\text{N}$ (for $R = 30 \mu\text{m}$, $h = 40 \mu\text{m}$, $\mu = 5 \text{ mPas}$). Note that Δu depends on α and that, given all the assumptions and simplifications made to arrive at Eq. (6), the values obtained for F_d should be considered an order of magnitude estimation.

At the highest sorting speeds, the condition of a constant velocity along the gap does not hold, and the drop will be pulled off the gap. For successful sorting, however, a drop only has to be deflected a small distance perpendicular to the flow direction to be sent into that particular outlet. Therefore, sorting can still be possible at slightly higher flowrates than our model predicts. Furthermore, even if $F_{e,max} \geq F_d \sin(\alpha)$, at high sorting speeds two drops or a drop and the wall can come close together, resulting in hydrodynamic interactions that make our model less predictive.

IV. RESULTS

All experiments showed that a 100% reliable sorting (all drops sorted as intended) could be achieved by increasing the voltage above a flowrate dependent threshold. Different sorting modes were explored.

In one series of experiments, the sorter was conditioned such that, without electrical actuation, all drops would leave the sorter via the same outlet. This was achieved by applying an excess pressure to the other outlet. For several combinations of oil and water flow rates, it was examined how the efficiency of sorting into the hydraulically disfavored outlet depended on the applied voltage. The amplitude of this continuously applied AC signal was increased stepwise until the efficiency had reached 100%. Per step, about 400 sorting events were recorded and analyzed with Matlab scripts. Besides counting the percentage of drops going into either outlet, also the injection frequency, size, and velocity of the drops were measured. The results are summarized in Table I and Fig. 4.

The minimum voltage required for 100% sorting increases both with Q_{oil} and with Q_{water} . This is in accordance with the expected dependence on the total flow rate: a larger Q_{total} implies a stronger drag force on the drop, which in turn implies that a stronger electrostatic force is needed to overcome this bias. Fig. 4 shows that for each experiment at fixed flow rates,

TABLE I. Electric sorting of water drops in FC40 oil, against a pressure bias, at different flow rates. From video analysis, the average drop generation frequency f_{drop} , average drop velocity v_{drop} , and the average drop radius R are determined. Also the inter-experimental standard deviation is determined. The last column shows the minimum voltage that is needed to change the destination of all drops from one outlet (in the absence of voltage) to the other. The number is obtained from a linear fit to the data shown in Fig. 4. Increasing flow rates require higher voltage to sort 100% of the drops.

Q_{oil} (ml/h)	Q_{water} (μ l/h)	f_{drop} (Hz)	v_{drop} (mm/s)	R (μ m)	$V_{100\% \text{ sorted}}$ (V)
2.0	70	175 ± 12	81 ± 6	33.7 ± 0.8	103
2.5	75	227 ± 17	110 ± 7	31.4 ± 0.6	111
2.5	150	422 ± 19	113 ± 8	32.1 ± 0.6	128
3.0	180	556 ± 32	141 ± 6	31.1 ± 0.5	139

the sorting efficiency increases gradually with the voltage. Closer inspection of the movies revealed that sometimes, an ongoing accumulation of subsequent drops in the same outlet channel, led to a favoring of the other channel. This is ascribed to the increase in hydraulic resistance as the outlet gets filled with drops. Most important for practical applications, however, is that the consistent 100% sorting percentage can be obtained by choosing just a small excess voltage over $V_{100\%}$.

The size distribution of the drops is monodisperse, as is usual for flow focusing devices. Using the maximum diameter $2R$ in a transmission image (e.g., Fig. 5) to characterize the drop size, we found the standard deviation to be $\sim 3\%$. To simplify the comparison between the experiments at different flow rates, we aimed to keep R constant. As Table I shows, an almost constant value of $32 \pm 2 \mu\text{m}$ could be achieved. Because the channel height was only $40 \mu\text{m}$, this implies that the drops are slightly flattened. The nearly constant R was achieved by setting the oil flow rate Q_{oil} much higher than the water flow rate Q_{water} . In this regime, the drop radius is mainly determined by the size of the orifice of the FFD. The drop volume, which shows a stronger dependence on R , is constant within $\sim 10\%$ between experiments. Mass conservation then dictates that the drop generation frequency f_{drop} (varied from 175 to 556 s^{-1}) should be proportional to Q_{water} within comparable accuracy; this appears to be the case. The drop velocity was measured to be proportional to the total flow rate; also this is in agreement with expectations.

In another set of experiments, the sorter was used without the pressure bias. In this mode, the sorter electrodes are always active, to ensure that all drops go into the “waste” outlet. Switching the center electrode allows to select one or multiple drops to sort towards the other outlet. Compared to the previous sorting mode, the required electrostatic force (at given flow rates) is lower. Because only small biases (like slight asymmetries in the channel structure, or

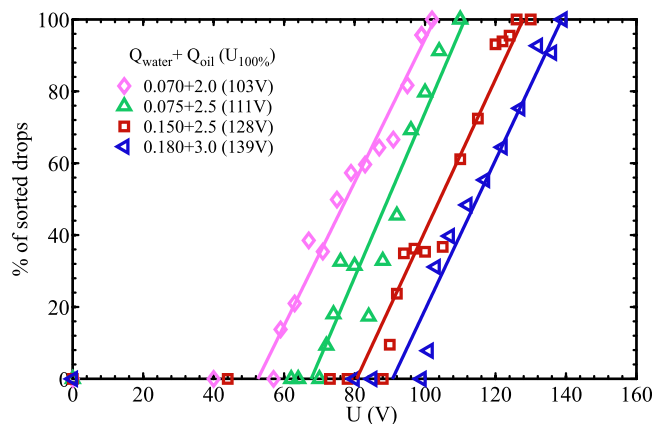


FIG. 4. Percentage of drops being actively sorted against the applied voltage for different water and (FC40) oil flow rate conditions in ml/h. Each data point is determined from a movie of ~ 400 drops.

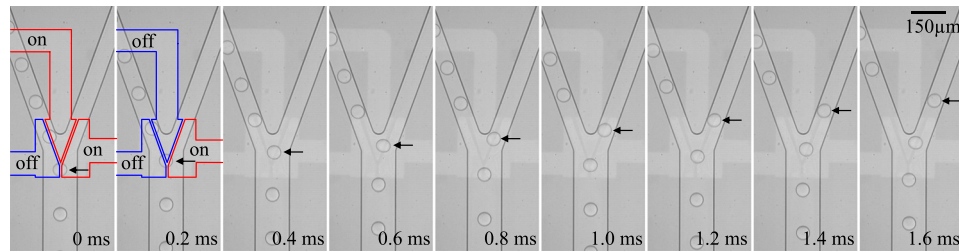


FIG. 5. A 1.6 ms interval of the sorting of water drops in FC40 at 1200 per second. At 0 ms, the center electrode is active, steering all drops to the left outlet. At 0.2 ms, the center electrode is switched off, resulting in drops going towards the right outlet. See movie 1 in supplementary material for water drops sorted at 1200 drops per second.²¹

the mentioned effect of downstream accumulation, or misalignment of the sorting electrodes beneath the channel) need to be overcome, the drops require only a small deflection to be steered into the correct channel. This should allow for faster sorting. To explore the limits in sorting rate, we first continued the experiments in FC-40 oil. Our protocol started with a maximization of the steering voltage; here, we found that an upper limit for the voltage is not posed because of dielectric breakdown, but is posed by an electrical instability of the contact line resulting in the ejection of small satellite drops.¹⁸ Using a typical $50 \text{ V}/\mu\text{m}$ limit, dielectric breakdown is estimated to occur around $300 V_{\text{RMS}}$ for the $3 \mu\text{m}$ dielectric. Experiments show that contact line instability occurs around $250 V_{\text{RMS}}$. After fixing the voltage, pressure control on the oil and water phases was used to find the maximum rate of drop formation that would still result in reliable sorting. We consider sorting reliable if all drops are steered into the desired outlet. Preliminary experiments showed that this condition is more difficult to achieve than other sorting protocols, such as alternately steering drops to the outlets.

We find that not the total flow rate, but the inter-drop distance ultimately limits the maximum sorting speed. At too high sorting rates, drops stagnate at the tip of the Y-channel junction. The distance between the stagnant and consecutive drop then becomes too small, forcing the latter towards the undesired outlet via hydrodynamic interaction. The best achievement obtained for drops with $R \sim 25 \mu\text{m}$ was a rate of 1200 s^{-1} , which is a considerable improvement as compared to 25 s^{-1} in an earlier device.¹² This experiment is shown in Fig. 5.

To inspect the role of the viscosity of the continuous phase, we also maximized the drop sorting rate for different oils. Although replacement of oil generally involves more changes than just the viscosity (e.g., also the interfacial tension), it was possible to make drops of a similar size ($R \sim 25 \mu\text{m}$) and hence obtain the same (expected) relation between the voltage and the electric sorting force. Moreover, by adapting Q_{water} to Q_{oil} , it was also possible to vary the overall flow rate while keeping the drop size constant. This allows quantitative comparison between the experiments and our model. According to the model, the maximum flow rate at which 100% sorting is still possible, should follow from a balance between the sorting force and the drag force. Keeping the maximum sorting force the same, it is then implied that the maximum sorting rate should be inversely proportional to the oil viscosity. Experiments with 3 different oils suggests that this is indeed the case: sorting rates were 1213/s for FC40 (5 mPa s), 175/s for light mineral oil (31.5 mPa s), and 30/s for paraffin oil (119 mPa s). These viscosity values are obtained experimentally at an ambient temperature of 21°C . Results are shown in Fig. 6.

To further examine the sorting process under conditions optimized for maximum rate, we consider how the magnitude and direction of the sorting force develop along the path of the sorted drop. Fig. 7 shows a representative case where the sorting rate is (almost) maximal. For each video frame, the electrostatic force on the drops can be estimated. For this, we first measure the electrode areas covered by each individual drop. To translate this into a force, we not only use a numerically calculated calibration function for $F_{el}(x)/cRU^2$ that is similar to the expression of Eq. (4) and the graph in Fig. 3 but also takes into account the finite gap between the electrodes. Use of the relation between x , the distance of center of mass to the electrode

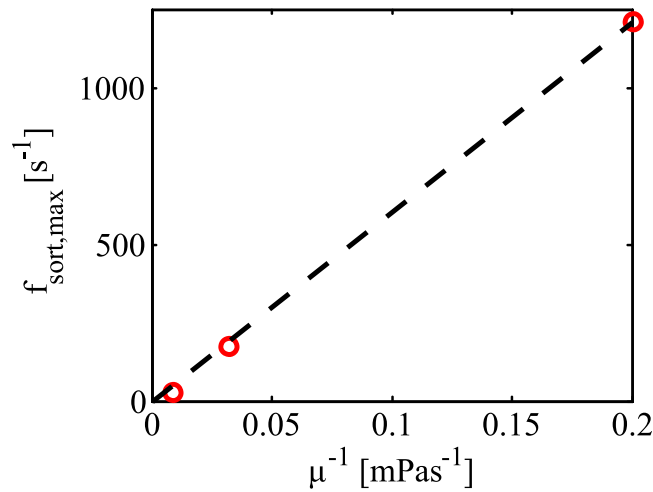


FIG. 6. The maximum sorting speeds achieved using oils of different viscosity ($\mu = 169, 32,$ and 5 mPa s). In all experiments, the channel geometry is the same, as well as the drop radius ($\sim 25 \mu\text{m}$). The electrostatic force is independent of viscosity, while the drag force is proportional to the viscosity. Therefore, the relation between maximum achievable sorting speed and reciprocal of the viscosity is close to linear.

gap, and A_1/A_2 for that case then allows to obtain the force from the measured areas. The underlying assumption that the drop footprint is circular is not met, because drops can deform under the influence of the electrostatic and drag force (as can be seen in Fig. 7). However, even an (estimated) error of 10%-20% still makes that the electrostatic force is known with much better accuracy than the hydrodynamic drag force as estimated via Eq. (6). While the electric and hydrodynamic forces are in the μN range, the inertial force can simply be verified to be in

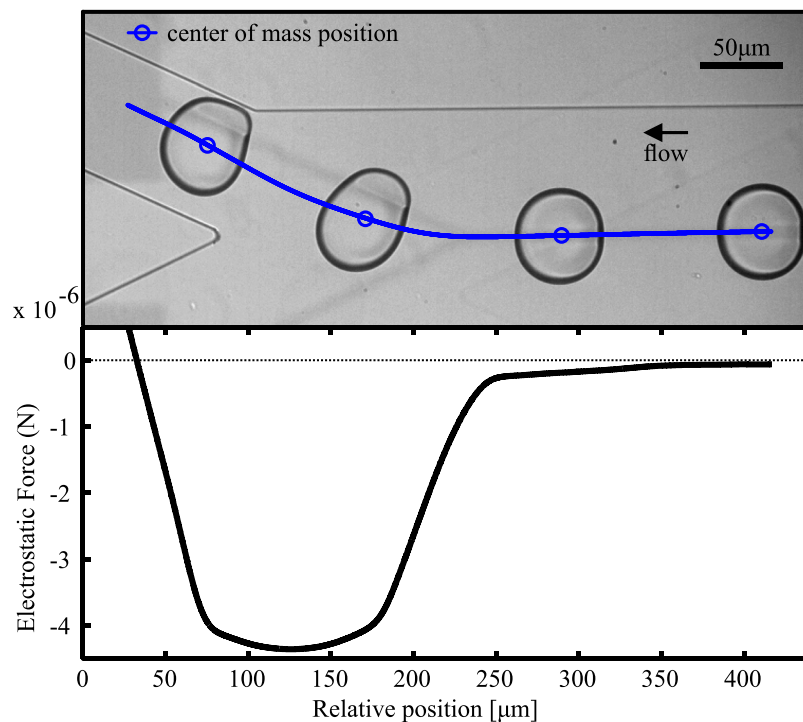


FIG. 7. Top: snapshot of four drops of KCl water dispersed in light mineral oil being sorted at 25 drops per second. Overlaid in blue: the averaged center of mass position of 27 consecutive drops undergoing sorting. Bottom: Graph of the averaged absolute electrostatic force on a series of 27 drops during sorting. See movie 2 in the supplementary material for the detection and measurement of drops during sorting and the resulting calculated electrostatic force.²¹

the pN range. This means that we can (i) calculate the drag force by equating it to the electrostatic force and (ii) compare it to the largest achievable electrostatic force. The comparison in Fig. 7 confirms that the electrostatic force exerted on the drop at the highest sorting rates is very close to the maximum value from our model. Conversely, a comparison with the drag force calculated via Eq. (6) suggests that the latter is underestimated by a factor of 4 by the model.

V. DISCUSSION

It is interesting to examine which processes posed limitations to the sorting rates that could be achieved. The drop generation frequency was not a limiting factor in this work. The maximum voltage in our experiments was determined by the intrinsic instability of the drop against ejection of satellite drops,¹⁸ not by dielectric breakdown. Since this problem is caused by an excessive local electric field at the drop contact line and the sorting force originates from the same field, this intrinsic limitation can only be improved by oil-water combinations with higher surface tension.

In our earliest channel designs, the tip of the Y-channel junction was very sharp, which led to drops being split at highest sorting rates. This problem was mitigated by giving the Y-junction a rounded corner (as in Fig. 5). However, this has the side effect of creating a wider stagnation zone at the junction of the outlet channels, where drops slow down as they near the channel wall. If the deflection of a drop is insufficient, this stagnation causes subsequent drops to approach each other too closely, leading either to coalescence or uncontrolled choice of the outlet channel by hydrodynamic interaction. This effect increases the required drop deflection for sorting, ultimately limiting the drop sorting frequency. To disfavor the close approach of the inner wall, the Y-shaped electrode geometry can be placed further away from Y-channel junction (see Fig. 7). Other biases, like an asymmetric presence of drops in either of the two outlets—causing a difference in hydraulic resistance—did not influence the sorting efficiency much in our experiments.

If the drag force becomes too large, the drops will no longer follow the electrode gap. In that case, a smaller opening angle of the sorter would be needed, as this shifts the force balance in favor of the electric force. However, this smaller angle would in turn require a longer distance between subsequent drops, since the active sorter should still be able to determine the fate of each individual drop. This issue can be remedied by adding two extra oil inlets just after the flow focusing junction, which increases the inter drop distance. This would, however, increase the drag force. In summary, it is not clear to what extent the handling speed of the present sorter could be further enhanced via geometric design.

Another aspect of practical relevance for any drop sorter is durability. While for each of the used oils the life time of the sorter was long enough to systematically explore the different voltages and flow rates, we did observe noteworthy differences in durability. Although each of the used oils shows similar wetting on PDMS (as was verified with experiments on PDMS slabs, where the contact angle of the water drop under the different oils is always larger than 160°), in a few cases, we found that drops had begun to wet the dielectric substrate at the electrodes, ultimately leading to failure of the device. The time before this happens showed strong variations: drops of PBS (Phosphate Buffer Saline) solution in light mineral oil could be sorted at 100 V for at least 72 h, without any noticeable detrimental effect on sorting, while drops of KCl solution in FC-40 oil could be sorted at maximum rate at 220 V only for 6 h. Additional diagnosis revealed that dielectric breakdown of the PDMS due to the applied voltage was not the cause of the degradation. The actual origin, however, could not be identified.

An explanation can be found by considering the oil film that separates the aqueous drop from the PDMS coating on the electrodes. If this film becomes too thin, direct contact of the drop can occur due to Van der Waals attraction, even though the Hamaker constants are small ($<2 \times 10^{21}$ J). The breakdown probability of the lubrication layer depends both on the film thickness and the “exposure time” of the drop to the electric field, i.e., the time needed for the drop to pass the electrode. Here, the electric field drives the thinning of the layer of oil, while

its viscosity influences the time scale of this process. The thickness h of a film subjected to an electric field is known to scale with the applied voltage as¹⁷

$$h \sim (d\sqrt{R})^{2/3} \left(\frac{Ca}{\eta} \right)^{2/3}, \quad (7)$$

where Ca is the capillary number

$$Ca = \frac{\mu v}{\gamma}, \quad (8)$$

with μ as the oil viscosity, γ as the oil/water interfacial tension, and η as the electrowetting number

$$\eta = \frac{\epsilon_0 \epsilon_r U^2}{2d\gamma}. \quad (9)$$

This suggests that, for a given drop radius R and insulator thickness d , the film thickness $h \propto Ca^{2/3} U^{-4/3}$. Therefore, three factors can promote the wetting of the substrate by water: a lower oil viscosity, a lower drop velocity, and a higher voltage. It is worthwhile to note that the capillary numbers for the maximum sorting speed experiments with different oils are the same, because γ remains ~ 50 mN/m, and μv is proportional to the drag force. Comparison between the before mentioned wetting case of FC-40 and the non-wetting mineral oil reveals that the FC-40 case indeed has a (sixteen times) thinner oil film.

Another aspect of durability is that also the content of the drop can favor wetting of the surface. In particular, amphiphilic biological molecules like proteins have a tendency to adsorb at the oil/water interface and subsequently at the channel walls, thereby making them hydrophilic. In our case, this was observed with Dulbecco's Modified Eagle Medium as the drop phase. However, this type of issue is not an inherent aspect of our sorter. Mitigations of this aspect are already known, e.g., by using specific surfactants to cover the interface of the drop¹⁹ or the channel walls.²⁰

VI. CONCLUSION

The present study demonstrates that simple design rules can be used to enhance the rate of drop sorting, when compared to an earlier prototype electrostatic sorter. The electrostatic force exerted by a coplanar electrode geometry can be controlled by both the geometry of the design (insulator thickness, electrode size, and gap width) and the applied voltage. An additional way to favor the balance between the steering (electrostatic) and the opposing (hydrodynamic) forces is to reduce the latter. Use of a low viscosity oil and a small opening angle of the sorter were both applied, and contributed to the achievement of sorting rates up to 1200/s for 160 pl drops. The use of smaller drops could be yet another way to increase the sorting rate, since this would lower the drag force more strongly than the steering force. Ultimately, the specific application will determine to what extent the various degrees of freedom can be used: for example, cells in drops might require specific drop volumes and (bio) compatible oils. We remark here that electrowetting sorters do not pose limitations to the drop sample material via electric fields: the sorting principle still works at physiological high salt concentrations, and the contents of the drop are not exposed to electric fields. The present work also showed that, although the proportionality of the drag force with drop velocity and oil viscosity provides a global design rule, an analytical estimate of this force is difficult to obtain, even if the presence of other nearby drops can be neglected.

Finally, we like to point out that from a practical point of view our sorter has the following advantages: (i) the fabrication costs are low, due to the use of standard PDMS and ITO electrodes, (ii) 100% reliability of sorting can be achieved for a wide range of flow rates, (iii) the

durability of the device is promising (evidenced by a sorting experiment that lasted 3 days), (iv) the sorting forces are strong (1000 times larger than reported in DEP sorting⁶ at a 10 times lower voltage), (v) sorting speeds exceeding 1 kHz can be reached, (vi) also sorting of highly conductive drops can be achieved, (vii) the drop contents are not exposed to electric fields or Joule heating (as in DEP), and (viii) the physical concepts are simple, which allows users to design their own electrode geometries for their specific application.

VII. FUTURE PROSPECTS

In preliminary sorting experiments of drops containing fluorescently labeled cells, we were able to separate cell-laden drops from empty ones by sorting at 400 drops per second. The use of a surfactant served to protect all interfaces from the adsorption of drop contents. The decreased oil-water surface tension did not negatively affect the sorting. Sensitive detection of the cells' fluorescence using a photomultiplier tube was used in combination with the speed of a Field Programmable Gate Array to trigger the amplifier of the steering signal at a rate that was so fast, in which the focal spot for the fluorescent excitation actually had to be placed just micrometers in front of the Y-junction. For a recording of this experiment, which underlines the potential of our method, see movie 3 in supplementary material for live sorting of cell containing drops at 400 drops per second.²¹

ACKNOWLEDGMENTS

This research was supported by the Dutch Technology Foundation STW, which is part of the Netherlands Organization for Scientific Research (NWO), and which is partly funded by the Ministry of Economic Affairs.

We like to thank Dr. Aigars Piruska and Professor Wilhelm T. S. Huck from the Physical-Organic Chemistry Group at the Radboud University (Netherlands) for performing the cell sorting experiments on their high speed fluorescence detection and actuation setup, as well as supplying fluorescently labeled cells and fluorinated surfactants.

- ¹A. B. Theberge, F. Courtois, Y. Schaerli, M. Fischlechner, C. Abell, F. Hollfelder, and W. T. Huck, *Angew. Chem.* **49**(34), 5846–5868 (2010).
- ²A. B. Theberge, E. Mayot, A. El Harrak, F. Kleinschmidt, W. T. Huck, and A. D. Griffiths, *Lab Chip* **12**(7), 1320–1326 (2012).
- ³A. R. Abate, C. H. Chen, J. J. Agresti, and D. A. Weitz, *Lab Chip* **9**(18), 2628–2631 (2009).
- ⁴E. W. Kemna, R. M. Schoeman, F. Wolbers, I. Vermes, D. A. Weitz, and A. van den Berg, *Lab Chip* **12**(16), 2881–2887 (2012).
- ⁵J. C. Baret, O. J. Miller, V. Taly, M. Ryckelynck, A. El-Harrak, L. Frenz, C. Rick, M. L. Samuels, J. B. Hutchison, J. J. Agresti, D. R. Link, D. A. Weitz, and A. D. Griffiths, *Lab Chip* **9**(13), 1850–1858 (2009).
- ⁶K. Ahn, C. Kerbage, T. P. Hunt, R. M. Westervelt, D. R. Link, and D. A. Weitz, *Appl. Phys. Lett.* **88**(2), 024104 (2006).
- ⁷T. Franke, A. R. Abate, D. A. Weitz, and A. Wixforth, *Lab Chip* **9**(18), 2625–2627 (2009).
- ⁸L. Wu, P. Chen, Y. Dong, X. Feng, and B. F. Liu, *Biomed. Microdevices* **15**(3), 553–560 (2013).
- ⁹B. Ahn, K. Lee, R. Panchapakesan, and K. W. Oh, *Biomicrofluidics* **5**(2), 024113 (2011).
- ¹⁰E. Fradet, C. McDougall, P. Abbyad, R. Dangla, D. McGloin, and C. N. Baroud, *Lab Chip* **11**(24), 4228–4234 (2011).
- ¹¹A. R. Abate, J. J. Agresti, and D. A. Weitz, *Appl. Phys. Lett.* **96**(20), 203509 (2010).
- ¹²R. de Ruiter, A. M. Pit, V. M. de Oliveira, M. H. G. Duits, D. van den Ende, and F. Mugele, *Lab Chip* **14**(5), 883–891 (2014).
- ¹³D. C. Duffy, J. C. McDonald, O. J. Schueller, and G. M. Whitesides, *Anal. Chem.* **70**(23), 4974–4984 (1998).
- ¹⁴D. 't Mannetje, S. Ghosh, R. Lagraauw, S. Otten, A. Pit, C. Berendsen, J. Zeegers, D. van den Ende, and F. Mugele, *Nat. Commun.* **5**, 3559 (2014).
- ¹⁵F. Mugele and J.-C. Baret, *J. Phys.: Condens. Matter* **17**(28), R705 (2005).
- ¹⁶D. 't Mannetje, A. Banpurkar, H. Koppelman, M. H. Duits, D. van den Ende, and F. Mugele, *Langmuir* **29**(31), 9944–9949 (2013).
- ¹⁷A. Staicu and F. Mugele, *Phys. Rev. Lett.* **97**(16), 167801 (2006).
- ¹⁸F. Mugele and S. Herminghaus, *Appl. Phys. Lett.* **81**(12), 2303–2305 (2002).
- ¹⁹J. C. Baret, *Lab Chip* **12**(3), 422–433 (2012).
- ²⁰J. W. Zhou, D. A. Khodakov, A. V. Ellis, and N. H. Voelcker, *Electrophoresis* **33**(1), 89–104 (2012).
- ²¹See supplementary material at <http://dx.doi.org/10.1063/1.4928452> for water drops sorted at 1200 drops per second (movie 1), for the detection and measurement of drops during sorting and the resulting calculated electrostatic force (movie 2), and for live sorting of cell containing drops at 400 drops per second (movie 3).